Density derivative-based approaches for overhang control in topology optimization in 3D-printing

Francesco Mezzadri[1]

University of Modena and Reggio Emilia, Department of Engineering "Enzo Ferrari"

INdAM Workshop "Mathematical Methods for Objects Reconstruction: from 3D Vision to 3D Printing"

Based on joint reasearch with Xiaoping Qian, University of Wisconsin - Madison (U.S.A.)

---

[1]francesco.mezzadri@unimore.it

Outline

We want overhang control: constraint based on first-order derivatives of density

However, oscillating boundaries may occur: measure and suppress them by second-order derivatives of density

Outline

We want overhang control: constraint based on first-order derivatives of density

However, oscillating boundaries may occur: measure and suppress them by second-order derivatives of density

Outline

We want overhang control: constraint based on first-order derivatives of density

However, oscillating boundaries may occur: measure and suppress them by second-order derivatives of density

Outline

We want overhang control: constraint based on first-order derivatives of density

However, oscillating boundaries may occur: measure and suppress them by second-order derivatives of density

Outline

We want overhang control: constraint based on first-order derivatives of density
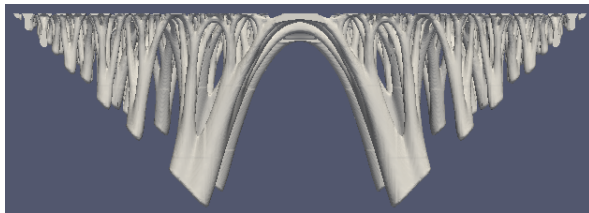
However, oscillating boundaries may occur: measure and suppress them by second-order derivatives of density

Topology optimization and 3D printing

Topology optimization allows to determine the optimal design to withstand a given set of loads.

The optimized design can, nonetheless, be complex and have fine features.

3D-printing is attractive to manufacture the optimized designs

Overhangs in 3D printing

Consider an additive manufacturing process that is performed along a given build direction b (e.g., the vertical axis). Let α denote the overhang angle.
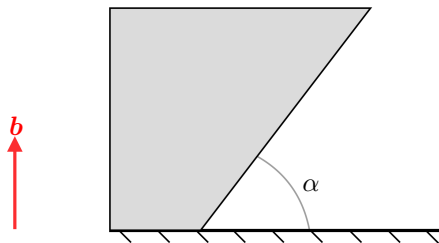

Figure: The overhang angle, where b is the build direction and α is the overhang angle

- if α sufficiently steep ➡ self-supporting;

- if α not steep enough ➡ structure may collapse during manufacturing.

- if α sufficiently steep ➡ self-supporting;

- if α not steep enough ➡ structure may collapse during manufacturing.

Add sacrificial support structures

Consider designs that are self-supporting

- if α sufficiently steep ➡ self-supporting;

- if α not steep enough ➡ structure may collapse during manufacturing.

Add sacrificial support structures
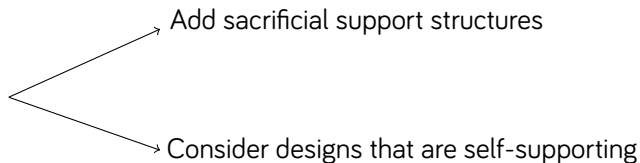
Consider designs that are self-supporting
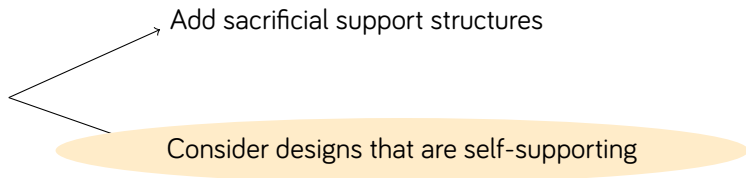
In topology optimization, we can forbid designs that are not self-supporting by filters or constraints.

The Projected Undercut Perimeter (PUP) constraint

The PUP constraint[2] is based on the analysis of the gradient of density. In particular, let γ be the design variable.

- $\nabla\gamma \neq 0$ only along the contour of the design;
- $\nabla\gamma \cdot \boldsymbol{b} > 0$ in overhanging boundaries.
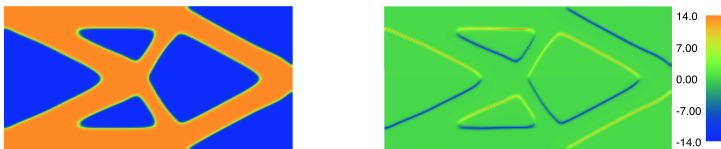
Figure: A design (left) and the directional derivative $\nabla\gamma \cdot \boldsymbol{b}$ (right)

[2]X. Qian. "Undercut and overhang angle control in topology optimization: A density gradient based integral approach". In: *International Journal for Numerical Methods in Engineering* 111.3 (2017), pp. 247–272.

Moreover, it is easy to correlate $\nabla\gamma \cdot \boldsymbol{b}$ to the overhang angle α by
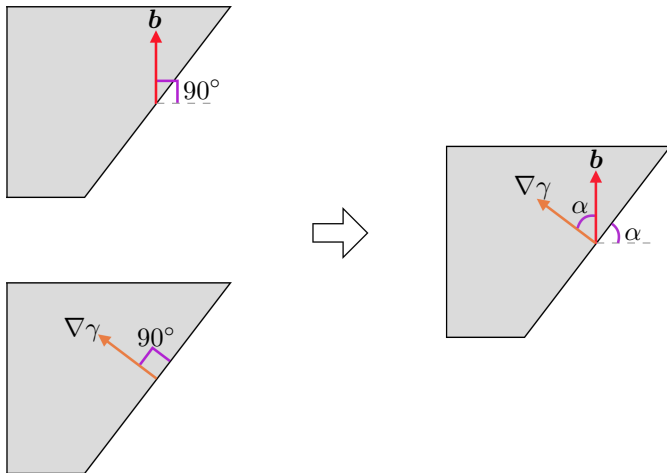
$$\frac{\nabla\gamma \cdot \boldsymbol{b}}{\|\nabla\gamma\|} = \cos(\alpha).$$

Then, if $\bar{\alpha}$ is a given threshold to the overhang angle, a boundary is self-supporting when

$$\frac{\nabla\gamma \cdot \boldsymbol{b}}{\|\nabla\gamma\|} \leq \cos(\bar{\alpha}).$$

The PUP constraint is based on imposing this condition by means of a (continuous and differentiable approximation of) Heaviside projection. By applying also a shifting,

$$H_{\bar{\alpha}}(\gamma) = H\Big(\frac{\nabla\gamma \cdot \boldsymbol{b}}{\|\nabla\gamma\|} - \cos(\bar{\alpha})\Big)$$

is a function which is nonzero only along boundaries which violate the self-support condition.

Then, if $\bar{\alpha}$ is a given threshold to the overhang angle, a boundary is self-supporting when

$$\frac{\nabla\gamma \cdot \boldsymbol{b}}{\|\nabla\gamma\|} \leq \cos(\bar{\alpha}).$$

The PUP constraint is based on imposing this condition by means of a (continuous and differentiable approximation of) Heaviside projection. By applying also a shifting,

$$H_{\bar{\alpha}}(\gamma) = H\Big(\frac{\nabla\gamma \cdot \boldsymbol{b}}{\|\nabla\gamma\|} - \cos(\bar{\alpha})\Big)$$

is a function which is nonzero only along boundaries which violate the self-support condition.

The projected overhang can thus be represented as

$$P_{\bar{\alpha}} = \int_{\Omega} H_{\bar{\alpha}}(\gamma)\nabla\gamma \cdot \boldsymbol{b}d\Omega$$

and the PUP constraint is formulated as

$$P_{\bar{\alpha}} \leq \bar{P}_{\bar{\alpha}},$$

where $\bar{P}_{\bar{\alpha}}$ is a given threshold to the overhanging perimeter where the overhang angle exceeds $\bar{\alpha}$.

Gradient-based overhang constraint

The projected overhang can thus be represented as

$$P_{\bar{\alpha}} = \int_{\Omega} H_{\bar{\alpha}}(\gamma) \nabla \gamma \cdot \boldsymbol{b} d\Omega$$

and the PUP constraint is formulated as

$$P_{\bar{\alpha}} \leq \bar{P}_{\bar{\alpha}},$$

where $\bar{P}_{\bar{\alpha}}$ is a given threshold to the overhanging perimeter where the overhang angle exceeds $\bar{\alpha}$.

Gradient-based overhang constraint

Geometrical constraints and boundary oscillations

Advantages PUP:

- Simple, and with direct geometrical meaning;
- It can be imposed by adding a single integral constraint to the TO problem.

Issue: The PUP constraint can be satisfied also by oscillating solid-void boundaries.

Figure: Comparison of designs obtained without (left) and with (right) PUP constraint

This issue characterizes geometrical overhang constraints[3].

[3]G. Allaire et al. "Structural optimization under overhang constraints imposed by additive manufacturing technologies". In: *Journal of Computational Physics* 351 (2017), pp. 295–328.

Analysis of oscillations

We need to explicitly forbid designs with boundary oscillations

⬇

We formulate a measure of boundary oscillations[4], which is nonzero only when oscillations are present

valley   top of a hole, geometrically identical to a valley

tip

---
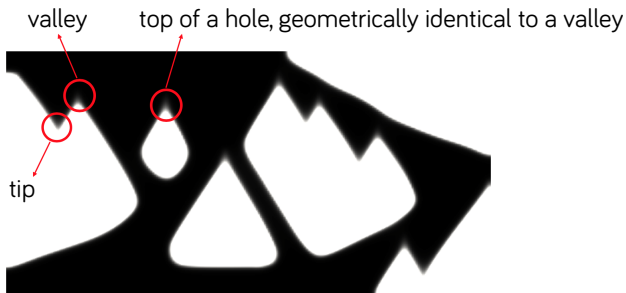
[4]F. Mezzadri and X. Qian. "A second-order measure of boundary oscillations for overhang control in topology optimization". In: *Journal of Computational Physics* 410, art. 109365 (2020), pp. 1–32.

Oscillations as maxima and minima

Let us analyze how γ evolves at a fixed height $\hat{z}$. The function

$$\Gamma(x) = \gamma(x, \hat{z})$$

describes how $\gamma(x, z)$ changes along x at $z = \hat{z}$.
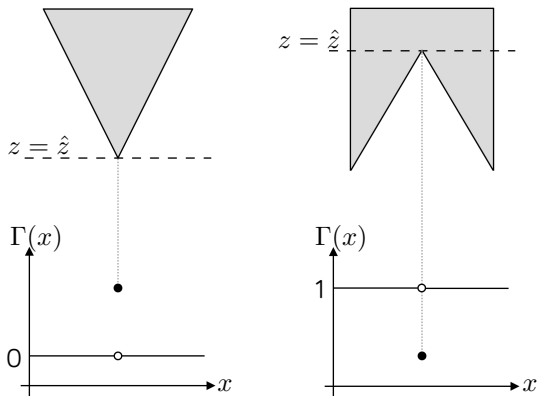
It is then easy to prove the following proposition:

Oscillations and second-order density derivatives

Let $(\hat{x}, \hat{z})$ be a point of the domain $\Omega \subset \mathbb{R}^2$ and let $\Gamma(x) = \gamma(x, \hat{z})$ be twice continuously differentiable in some neighborhood $\mathcal{I}(\hat{x})$ with $\Gamma''(\hat{x}) \neq 0$. Then, if $(\hat{x}, \hat{z})$ is the tip of an oscillation, the condition
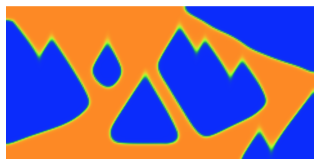
$$\Gamma''(\hat{x}) = \frac{\partial^2 \gamma(\hat{x}, \hat{z})}{\partial x^2} < 0$$
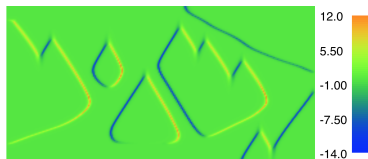
must be satisfied.
Similarly, if $(\hat{x}, \hat{z})$ is the valley of an oscillation or a pointy horizontal overhang, the condition

$$\Gamma''(\hat{x}) = \frac{\partial^2 \gamma(\hat{x}, \hat{z})}{\partial x^2} > 0$$

must be satisfied.

(a) Design

(b) $\dfrac{\partial \gamma(x, z)}{\partial x}$

(c) $\dfrac{\partial^2 \gamma(x, z)}{\partial x^2}$

(d) $\min\left(0, \dfrac{\partial^2 \gamma(x, z)}{\partial x^2}\right)$

Figure: Derivatives of γ with respect to x differentiate tips from valleys in an oscillating design

A characterization of tips of boundary oscillations

Second-order density derivatives are non-zero in various parts of the boundary.

However, tips of boundary oscillations are all facing directly downwards.

In all these points, we have

$$\|\nabla\gamma\| = \frac{\partial\gamma}{\partial z}.$$

Characterization of tips of boundary oscillations

Let $\gamma(x, z)$ be defined on the domain $\Omega \subset \mathbb{R}^2$. Furthermore, let $\gamma(x, z)$ be twice continuously differentiable on Ω and assume that oscillations are aligned along the z-axis. If a point $(\hat{x}, \hat{z}) \in \Omega$ satisfies

$$\|\nabla\gamma(\hat{x}, \hat{z})\| = \frac{\partial\gamma(\hat{x}, \hat{z})}{\partial z} \quad \text{and} \quad \frac{\partial^2\gamma(\hat{x}, \hat{z})}{\partial x^2} < 0,$$

then $(\hat{x}, \hat{z})$ is the tip of an oscillation.

A characterization of tips of boundary oscillations

Second-order density derivatives are non-zero in various parts of the boundary.

However, tips of boundary oscillations are all facing directly downwards.

In all these points, we have

$$\|\nabla\gamma\| = \frac{\partial\gamma}{\partial z}.$$

Characterization of tips of boundary oscillations

Let $\gamma(x, z)$ be defined on the domain $\Omega \subset \mathbb{R}^2$. Furthermore, let $\gamma(x, z)$ be twice continuously differentiable on Ω and assume that oscillations are aligned along the z-axis. If a point $(\hat{x}, \hat{z}) \in \Omega$ satisfies

$$\|\nabla\gamma(\hat{x}, \hat{z})\| = \frac{\partial\gamma(\hat{x}, \hat{z})}{\partial z} \quad \text{and} \quad \frac{\partial^2\gamma(\hat{x}, \hat{z})}{\partial x^2} < 0,$$

then $(\hat{x}, \hat{z})$ is the tip of an oscillation.

More in general, for an arbitrary build direction, we obtain the conditions

$$\frac{\nabla\gamma(\hat{x}, \hat{z}) \cdot \boldsymbol{b}}{\|\nabla\gamma(\hat{x}, \hat{z})\|} = 1 \quad \text{and} \quad q(\gamma) < 0,$$

where

$$q(\gamma) = \boldsymbol{b}_\perp^T \cdot \nabla^2\gamma(\hat{x}, \hat{z}) \cdot \boldsymbol{b}_\perp.$$

We can write a derivative-based measure to detect tips of oscillating boundaries

More in general, for an arbitrary build direction, we obtain the conditions

$$\frac{\nabla\gamma(\hat{x}, \hat{z}) \cdot \boldsymbol{b}}{\|\nabla\gamma(\hat{x}, \hat{z})\|} = 1 \quad \text{and} \quad q(\gamma) < 0,$$

where

$$q(\gamma) = \boldsymbol{b}_{\perp}^{T} \cdot \nabla^{2}\gamma(\hat{x}, \hat{z}) \cdot \boldsymbol{b}_{\perp}.$$

We can write a derivative-based measure to detect tips of oscillating boundaries

The second-order measure of boundary oscillations

Thus, we formulate the measure

$$m(\gamma) = q(\gamma)H_\theta(\gamma)\nabla\gamma \cdot \boldsymbol{b}$$

The second-order measure of boundary oscillations

Thus, we formulate the measure

$$m(\gamma) = \boxed{q(\gamma)} \; H_\theta(\gamma)\nabla\gamma \cdot \boldsymbol{b}$$

$\longrightarrow$ Negative at tips, positive at valleys

The second-order measure of boundary oscillations

Thus, we formulate the measure

$$m(\gamma) = q(\gamma) \; H_\theta(\gamma) \; \nabla\gamma \cdot \boldsymbol{b}$$

Nonzero only in horizontal overhangs

The second-order measure of boundary oscillations

Thus, we formulate the measure

$$m(\gamma) = q(\gamma)H_\theta(\gamma) \quad \nabla\gamma \cdot \boldsymbol{b}$$

↘ Detects boundaries sharply

The second-order measure of boundary oscillations

Thus, we formulate the measure

$$m(\gamma) = q(\gamma)H_\theta(\gamma) \quad \nabla\gamma \cdot \boldsymbol{b}$$

↘ Detects boundaries sharply

⬇

$m(\gamma)$ is negative only at tips of boundary oscillations

$$\hat{m}(\gamma) = \max(0, -m(\gamma))$$

or, in practice, the differentiable approximation

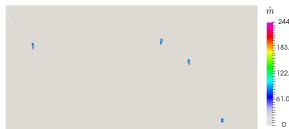$$\tilde{m}(\gamma) = -\frac{m(\gamma)}{1 + e^{\beta m(\gamma)}}$$

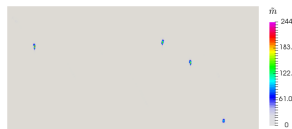are larger than zero only at tips of boundary oscillations.

(a) Design
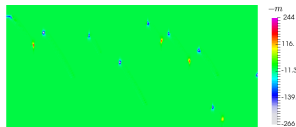
(b) $-m(\gamma)$

(c) $\hat{m}(\gamma)$

(d) $\tilde{m}(\gamma)$

Boundary oscillation control

Using $m(\gamma)$ we can develop several strategies to control boundary oscillations.

For instance,

1. We can suppress boundary oscillations by an adaptive PDE filter, whose (possibly anisotropic) radius is chosen based on $\hat{m}(\gamma)$

    We limit the disadvantages of large filter radius

2. We can formulate explicit constraints or cost penalizations

    We directly impose that $\tilde{m}(\gamma)$ sufficiently small

Boundary oscillation control

Using $m(\gamma)$ we can develop several strategies to control boundary oscillations.

For instance,

1. We can suppress boundary oscillations by an adaptive PDE filter, whose (possibly anisotropic) radius is chosen based on $\hat{m}(\gamma)$

   ⬇

   We limit the disadvantages of large filter radius

2. We can formulate explicit constraints or cost penalizations

   ⬇

   We directly impose that $\tilde{m}(\gamma)$ sufficiently small

Boundary oscillation control

Using $m(\gamma)$ we can develop several strategies to control boundary oscillations.

For instance,

① We can suppress boundary oscillations by an adaptive PDE filter, whose (possibly anisotropic) radius is chosen based on $\hat{m}(\gamma)$

We limit the disadvantages of large filter radius

② We can formulate explicit constraints or cost penalizations

We directly impose that $\tilde{m}(\gamma)$ sufficiently small

Generalities of adaptive filter

We compute

$$\widehat{M} = \int_\Omega \hat{m}(\gamma)d\Omega$$

If $\widehat{M}$ is above or below given thresholds, the filter radius (possibly only along a single direction) is increased or reduced locally.

In particular,

- If $\widehat{M}$ is large, then boundary oscillations are present

    the radius is increased along downward-facing boundaries

- If $\widehat{M}$ is close to zero, then boundary oscillations are not present

    we can reduce the filter radius everywhere, to obtain sharper designs

We can use the non-differentiable $\hat{m}(\gamma)$ because sensitivities are not needed.

Generalities of adaptive filter

We compute

$$\widehat{M} = \int_\Omega \hat{m}(\gamma) d\Omega$$

If $\widehat{M}$ is above or below given thresholds, the filter radius (possibly only along a single direction) is increased or reduced locally.

In particular,

- If $\widehat{M}$ is large, then boundary oscillations are present

  the radius is increased along downward-facing boundaries

- If $\widehat{M}$ is close to zero, then boundary oscillations are not present

  we can reduce the filter radius everywhere, to obtain sharper designs

We can use the non-differentiable $\hat{m}(\gamma)$ because sensitivities are not needed.

Outline of cost penalization

$\tilde{m}(\gamma)$ is nonnegative, its p-norm can be written as

$$\widetilde{M} = \Big(\int_\Omega \tilde{m}(\gamma)^p d\Omega \Big)^{1/p}.$$

We impose that $\widetilde{M}$ is small by constraints or cost penalization

Our implementation:

1. Set p large, so that $\widetilde{M}$ approximates the uniform norm of $\tilde{m}(\gamma)$;

2. Add $\widetilde{M}$ to the cost, applying also a weight w

In this context we use $\tilde{m}(\gamma)$, which is differentiable. We can then compute sensitivities.

Outline of cost penalization

$\tilde{m}(\gamma)$ is nonnegative, its p-norm can be written as

$$\widetilde{M} = \Big(\int_\Omega \tilde{m}(\gamma)^p d\Omega \Big)^{1/p}.$$

We impose that $\widetilde{M}$ is small by constraints or cost penalization

Our implementation:

1. Set p large, so that $\widetilde{M}$ approximates the uniform norm of $\tilde{m}(\gamma)$;

2. Add $\widetilde{M}$ to the cost, applying also a weight w

In this context we use $\tilde{m}(\gamma)$, which is differentiable. We can then compute sensitivities.

Oscillations in 3D domains

In 3D, we can still interpret tips of boundary oscillations as local maxima.
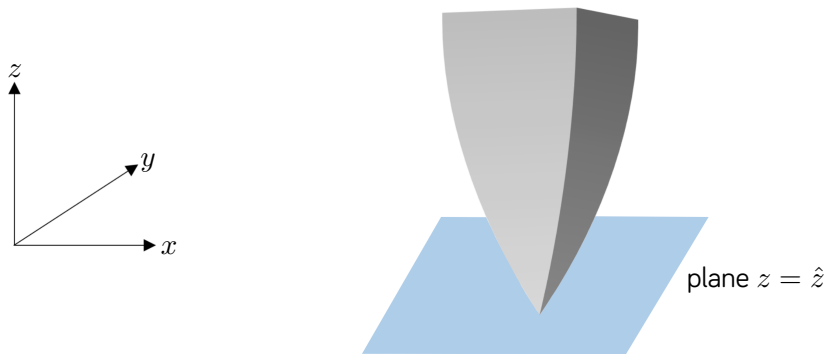
Figure: A boundary oscillation in 3D space

Thus, we just have to consider maxima on planes instead that in one dimension.

> ### Characterization of boundary oscillations in 3D
>
> Let $\gamma(x, y, z)$ be defined on the domain $\Omega \subset \mathbb{R}^3$. Furthermore, let $\gamma(x, y, z)$ have continuous second-order partial derivatives on Ω and assume that boundary oscillations are downward-facing. Finally, define $\Gamma(x, y) = \gamma(x, y, \hat{z})$. Then, if a point $(\hat{x}, \hat{y}, \hat{z}) \in \Omega$ satisfies
> $$\|\nabla \gamma(\hat{x}, \hat{y}, \hat{z})\| = \frac{\partial \gamma(\hat{x}, \hat{y}, \hat{z})}{\partial z} \quad \text{and} \quad \nabla^2 \Gamma(\hat{x}, \hat{y}) \prec 0,$$
>
> $(\hat{x}, \hat{y}, \hat{z})$ is the tip of a boundary oscillation.

The sign of the (2×2) Hessian matrix is studied by considering the sign of its minors, which involve the sign of the second-order derivatives of γ w.r.t. x and y.

Numerical experiments
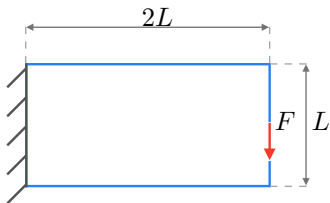
(a) 2D cantilever beam problem
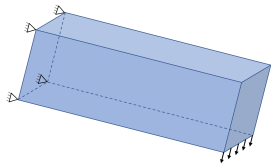
(b) 3D cantilever beam problem

Figure: Domain and boundary conditions of the considered problems
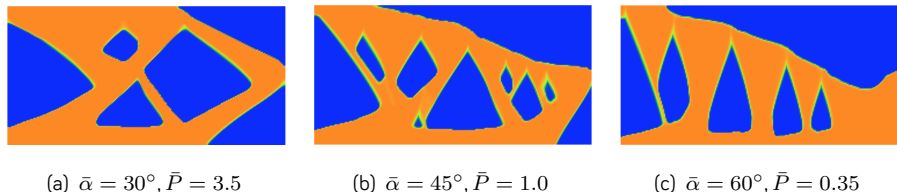
2D results with adaptive filter
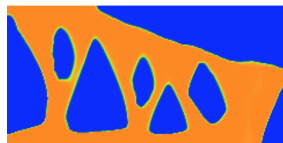

(a) $\bar{\alpha} = 30°, \bar{P} = 3.5$ (b) $\bar{\alpha} = 45°, \bar{P} = 1.0$ (c) $\bar{\alpha} = 60°, \bar{P} = 0.35$

Figure: Optimized designs for various choices of critical overhang angle $\bar{\alpha}$

Table: Cost of the designs, corresponding to different overhang angles $\bar{\alpha}$.

$\bar{\alpha}$	c	δc	M_{nd}
$30°$	62.70	9.1%	3.6%
$45°$	76.64	20.1%	6.4%
$60°$	109.58	38.6%	5.8%

2D results with cost penalization

(a) $\bar{\alpha} = 30°, \bar{P} = 1.5$ (b) $\bar{\alpha} = 45°, \bar{P} = 5.0$ (c) $\bar{\alpha} = 60°, \bar{P} = 3.0$

Figure: Optimized designs for various choices of critical overhang angle $\bar{\alpha}$

Table: Cost of the designs, corresponding to different overhang angles $\bar{\alpha}$.

$\bar{\alpha}$	c	δc	M_{nd}
$30°$	69.52	-0.8%	4.9%
$45°$	71.11	25.8%	4.2%
$60°$	89.59	46.4%	6.1%

Analysis of the 3D problem

Also in the considered 3D example, the PUP constraint can produce oscillating boundaries. The 3D measure can be used to detect them.
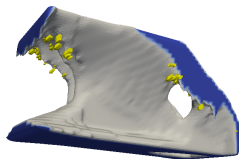
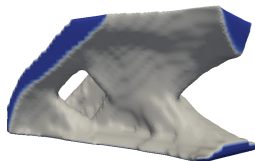(a) Measure of boundary oscillations over a view of the design
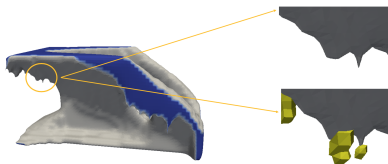
(b) Zoom-in of the measure of boundary oscillations in an oscillating boundary

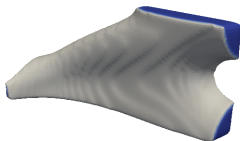Figure: The measure of boundary oscillations detects 3D oscillating boundaries

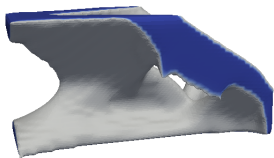# Results with adaptive filter
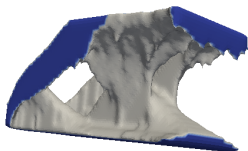
(a) Without adaptive filter. Cost: 41,382

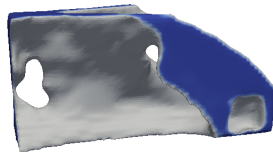(b) With adaptive filter. Cost: 42,852

(c) Witout adaptive filter, large radius. Cost: 64,989

Figure: Comparison between adaptive and non-adaptive filters of different radii.
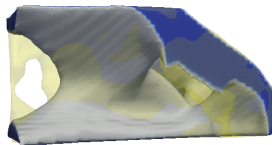
Results with cost penalization

(a) Unconstrained

(b) With oscillation penalty

(c) Design of point c (in yellow) over unconstrained

Figure: Results with cost penalization

An application in optimization of support structures

In some cases, a specific design must be manufactured, and it cannot be changed.

Support structures are needed.

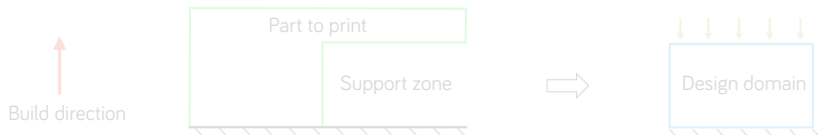In this case, it is possible to compute optimized support structures by solving a topology optimization problem[5].

Figure: Setting of the problem for support optimization

---

[5] F. Mezzadri, V. Bouriakov, and X. Qian. "Topology optimization of self-supporting support structures for additive manufacturing". In: *Additive Manufacturing* 21 (2018), pp. 666–682.

An application in optimization of support structures

In some cases, a specific design must be manufactured, and it cannot be changed.

Support structures are needed.

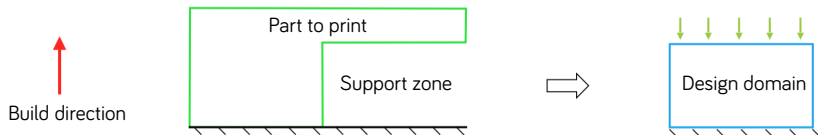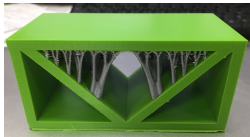In this case, it is possible to compute optimized support structures by solving a topology optimization problem[5].

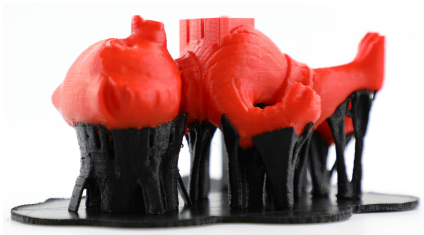Figure: Setting of the problem for support optimization

---

[5] F. Mezzadri, V. Bouriakov, and X. Qian. "Topology optimization of self-supporting support structures for additive manufacturing". In: *Additive Manufacturing* 21 (2018), pp. 666–682.

(a) A supported MBB beam
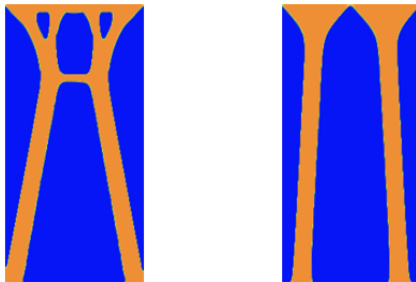

(b) A supported dome

(c) A supported complex structure

Figure: Some examples of optimized support structures

The proposed approaches can be useful also in the optimization of support structures.

Indeed, optimized supports structures can, in some cases, not be self supporting. Overhang control may then be required.

(a) Supports without overhang constraint
(b) Supports with overhang constraint

Figure: Comparison of optimized supports with and without overhang control

Conclusions

1. Approaches based on derivatives of the density function can be effectively used to detect overhangs and boundary oscillations;

2. Then, they allow to implement overhang control strategies for topology optimization in 3D printing;

3. The derivative-based measures allow to formulate various filters, constraints and penalizations;

4. Numerical results show the actual applicability of these procedures, also for 3D problems.

References

1. F. Mezzadri and X. Qian. "A second-order measure of boundary oscillations for overhang control in topology optimization". In: *Journal of Computational Physics* 410, art. 109365 (2020), pp. 1–32

2. F. Mezzadri, V. Bouriakov, and X. Qian. "Topology optimization of self-supporting support structures for additive manufacturing". In: *Additive Manufacturing* 21 (2018), pp. 666–682

3. X. Qian. "Undercut and overhang angle control in topology optimization: A density gradient based integral approach". In: *International Journal for Numerical Methods in Engineering* 111.3 (2017), pp. 247–272